

**Dependence of magnetism on GdFeO<sub>3</sub> distortion in the  $t_{2g}$  system  $ARuO_3$  ( $A = \text{Sr, Ca}$ )**Srimanta Middey,<sup>1</sup> Priya Mahadevan,<sup>2,\*</sup> and D. D. Sarma<sup>3</sup><sup>1</sup>*Centre for Advanced Materials, Indian Association for the Cultivation of Science, Jadavpur, Kolkata-700032, India*<sup>2</sup>*S.N. Bose National Centre for Basic Sciences, JD-Block, Sector III, Salt Lake, Kolkata-700098, India*<sup>3</sup>*Solid State and Structural Chemistry Unit, Indian Institute of Science, Bangalore-560012, India*

(Received 1 June 2010; revised manuscript received 12 October 2010; published 18 January 2011)

We have examined the stability of the ferromagnetic (FM) state in CaRuO<sub>3</sub> and SrRuO<sub>3</sub> as a function of the GdFeO<sub>3</sub> distortion. Model calculations predict the dependence of the FM transition temperature ( $T_c$ ) on the rotation angle  $\theta$  to vary as  $\cos^2(2\theta)$  for  $e_g$ -electron systems. However, here, we find an initial increase and then the expected decrease. Furthermore, a much faster decrease is found than predicted for  $e_g$ -electron systems. Considering the specific case of CaRuO<sub>3</sub>, a larger deviation of the Ru-O-Ru angle from 180° in CaRuO<sub>3</sub> as compared to SrRuO<sub>3</sub> should result in a more reduced bandwidth, thereby making the former more correlated. The absence of long-range magnetic order in the more correlated CaRuO<sub>3</sub> is traced to the strong collapse of various exchange interaction strengths that arises primarily from the volume reduction and increased distortion of the RuO<sub>6</sub> octahedra network that accompanies the presence of a smaller ion at the A site.

DOI: [10.1103/PhysRevB.83.014416](https://doi.org/10.1103/PhysRevB.83.014416)

PACS number(s): 75.10.-b, 75.30.Et, 71.20.-b

**I. INTRODUCTION**

As one goes down the periodic table from the 3d transition metal oxides to the 4d transition metal oxides, one finds fewer examples of magnetic materials. This is because the wider bands formed by the 4d compounds do not allow a local magnetic moment to be sustained in most cases. SrRuO<sub>3</sub> is a less commonly encountered example of a 4d oxide which is ferromagnetic. It has a transition temperature  $T_c$  of  $\sim 160$  K with a large magnetic moment of  $1.4 \mu_B$  per formula unit and is metallic down to low temperatures.<sup>1</sup> In the series Sr<sub>1-x</sub>Ca<sub>x</sub>RuO<sub>3</sub>, when one replaces Sr<sup>2+</sup> by a smaller cation Ca<sup>2+</sup>, the  $T_c$  decreases monotonically.<sup>2</sup> For CaRuO<sub>3</sub>, the magnetic ground state at low temperature has been controversial. Some people suggest an antiferromagnetic ordering of the spins at low temperature.<sup>3</sup> Some other people suggest absence of any ordering down to the lowest temperature studied.<sup>4</sup>

The origin of the different magnetic ground states for CaRuO<sub>3</sub> and SrRuO<sub>3</sub> has been a puzzle. Ca, being a smaller ion, should result in a more distorted perovskite structure than SrRuO<sub>3</sub>. This is indeed what is observed experimentally.<sup>5,6</sup> The Ru-O-Ru angle in SrRuO<sub>3</sub> is 166.0° in the ac plane and 170.0° along the b direction, while it is reduced to 151.1° in the ac plane and 150.7° along the b direction for CaRuO<sub>3</sub> (both in Pnma settings). The reduction in the Ru-O-Ru angle should result in a more reduced bandwidth for CaRuO<sub>3</sub> than SrRuO<sub>3</sub>. As one does not expect a significant change in U between the two systems,<sup>7</sup> these structural distortions should place the U : W ratio for CaRuO<sub>3</sub> to be larger than SrRuO<sub>3</sub> (i.e., making it more correlated). This would suggest that a magnetic ground state would be more favorable in CaRuO<sub>3</sub> than SrRuO<sub>3</sub>. Other effects such as the smaller volume of CaRuO<sub>3</sub> compared to SrRuO<sub>3</sub> work in increasing the bandwidth for CaRuO<sub>3</sub> and weaken the effects of correlation. There are indications from experiment, however, of CaRuO<sub>3</sub> being more correlated. The enhancement in the electronic specific heat coefficient over the band structure value is larger in CaRuO<sub>3</sub> than in SrRuO<sub>3</sub>. However, as mentioned earlier, there is no long-range magnetic order in CaRuO<sub>3</sub>. An additional puzzling aspect is that the magnetic moment is smaller in the more correlated CaRuO<sub>3</sub>.

The issue of absence of magnetic ordering in CaRuO<sub>3</sub> has been addressed earlier in the literature. First principle electronic structure calculations have been performed within density functional theory and have been found to capture the experimental trends.<sup>8-10</sup> However, the microscopic considerations that drive this are lost in such calculations. The difference in magnetic properties is attributed to the structural differences, primarily the Ru-O-Ru angle. This immediately raises the question, how does magnetic stability depend on the GdFeO<sub>3</sub> distortion angle in the  $t_{2g}$  system? In a system where the orbitals at the fermi level are  $e_g$  orbitals, an analytical expression exists. The magnetic stability is found to vary as  $\cos^2(2\theta)$ , where  $(180^\circ - 2\theta)$  is the TM-O-TM angle.<sup>11</sup> We set out by examining whether a similar dependence in the perovskite ruthenates is responsible for placing CaRuO<sub>3</sub> at a point where magnetism gets destabilized. The dependence of the magnetic stability on angle, we find is nonmonotonic. Surprisingly, there is an initial increase in the  $T_c$  and then a decrease as a function of angle. This is traced to the increase in bond length that takes place when the cubic perovskite is subject to a GdFeO<sub>3</sub> distortion. We have a low-spin system here, with  $t_{2g}$  down-spin levels being filled up after the up-spin levels are occupied. So with an increase in the bond length, there is an increase in the exchange splitting in the  $t_{2g}$  state which results in the initial increase in  $T_c$ . With larger changes in the angle, the distortion-induced reduction in the effective hopping between neighboring Ru atoms dominates, and  $T_c$  decreases. However, the rotation angle corresponding to the observed value is by itself insufficient to destabilize long-range magnetic ordering and a part of the destabilization is traced to the volume reduction that accompanies placing a smaller ion at the A site of the perovskite structure.

**II. METHODOLOGY**

The electronic structure of SrRuO<sub>3</sub> and CaRuO<sub>3</sub> was calculated using VASP, a plane wave pseudopotential implementation of density functional theory.<sup>12</sup> Projected augmented wave (PAW) potentials<sup>13</sup> were used along with the generalized gradient approximation (GGA) for the exchange. GGA calculations

were found to be adequate in getting a correct description of the ground state as GGA + U calculations showed a tendency of overemphasizing magnetism when applied to CaRuO<sub>3</sub>. In spite of the fact that the spin-orbit interaction is large in the case of the ruthenates, the effect of including spin-orbit interaction was found not to change the relative energy differences between the different magnetic states. The experimental crystal structures for CaRuO<sub>3</sub> and SrRuO<sub>3</sub> were taken from Refs.5,6. The lattice constants were kept fixed at the experimental values, while the internal coordinates were optimized to minimum energy configurations. Total energies for ferromagnetic, nonmagnetic, and different types of antiferromagnetic (A, C, G type)<sup>14</sup> spin configurations were calculated by integrating over a mesh of  $6 \times 6 \times 6$  K points over the complete brillouin zone. In order to understand the experimental trends in magnetism, we carried out total energy calculations for certain representative situations. An ideal perovskite unit cell for SrRuO<sub>3</sub> was considered with four formula units ( $\sqrt{2}a \times \sqrt{2}a \times 2a$ ) to treat all magnetic configurations considered earlier. The Ru-O-Ru angle was fixed at 180° and the lattice constant was varied and the changes in magnetic stabilization energy with volume was examined. We then studied the changes as a function of the Ru-O-Ru angle. Again four formula units were considered. The distortion was simulated by rotating each successive octahedron clockwise or anticlockwise by an angle  $\theta$  with respect to the 110 direction. The variation of the magnetic stabilization energies with  $\theta$  have been mapped on to a classical Heisenberg model of the form  $-\sum_{ij} J_{ij} e_i \cdot e_j$ . Here  $e_i, e_j$  are the unit vectors representing the direction of the spin.<sup>15</sup> This is because our earlier analysis showed that the magnitude of the spin was sensitive to the underlying magnetic configuration.<sup>16</sup> The exchange interactions  $J_{ij}$  entering the Heisenberg Hamiltonian were determined from the differences of energy for different spin configurations, and included up to second neighbor.

### III. RESULT AND DISCUSSIONS

In Table I we list the energies for SrRuO<sub>3</sub> and CaRuO<sub>3</sub> in different magnetic configurations for the optimized experimental structure. In SrRuO<sub>3</sub>, the ferromagnetic state is strongly stabilized by 25 meV per formula unit compared to the closest lying antiferromagnetic state which is the A-type antiferromagnetic state. For CaRuO<sub>3</sub> on the other hand, all magnetic configurations are found to lie close in energy, within the error bar of our calculations. In order to investigate whether this result had anything specifically to do with which atom we

had at the A site, we carried out calculations for CaRuO<sub>3</sub> in the SrRuO<sub>3</sub> relaxed experimental structure and vice versa. As is evident from the result shown in Table I, the magnetic stabilization energies found are independent of the atoms at the A site. This suggests that the different behavior we find for CaRuO<sub>3</sub> and SrRuO<sub>3</sub> arises from the differences in the crystal structure.

The first difference between the two systems arises from the difference in the volume. Ca is a smaller ion than Sr and so occupies a smaller volume. We first considered an ideal perovskite unit cell of SrRuO<sub>3</sub> and examine the stability of magnetic as well as the nonmagnetic state as a function of volume. A collapse of all magnetic configurations was found at small volumes as shown in Fig. 1(a). The reason for this is because, as the bond length is decreased, the hopping interaction strength between Ru  $d$  states and O  $p$  states increases. In the up-spin channel, both the Ru  $d$ -O  $p$  bonding and antibonding states of  $t_{2g}$  symmetry are occupied. However, in the down-spin channel, the antibonding states (primarily Ru  $d$  character) are partially occupied. With an increase in the hopping, one has an enhanced Ru  $d$  down-spin contribution in the occupied states, as a result of which the Ru  $d$  exchange splitting decreases. This results in the collapse of different magnetic configurations at smaller volumes. For better visual clarity, we plot the energy difference between the FM as well as the competing AFM state [inset of Fig. 1(a)] as well as replot Fig. 1(a) with all magnetic energies referenced to the energy of the nonmagnetic configuration [Fig. 1(b)]. The results of Table I suggest that for a given structure, the magnetic stabilization trends are independent of the choice of atom at the A site. So, we can infer what is expected for CaRuO<sub>3</sub> in the ideal structure, by examining the results for the volume corresponding to that of CaRuO<sub>3</sub>. Indeed the smaller volume of CaRuO<sub>3</sub> as compared to SrRuO<sub>3</sub> results in decreased magnetic stabilization energies for CaRuO<sub>3</sub>. However, the volume change is not enough to entirely destabilize the ferromagnetic state. The volume effect also explains the smaller magnetic moment found for CaRuO<sub>3</sub> compared to SrRuO<sub>3</sub> in experiments. In addition we have also considered the CaRuO<sub>3</sub> experimental structure and increased its volume by 5%. There we find that the ferromagnetic state is stabilized.

The small size of the Ca ion at the A site of the perovskite lattice results in a smaller volume for the CaRuO<sub>3</sub> unit cell than what one finds in SrRuO<sub>3</sub>. This would result in shorter Ru-O bonds for CaRuO<sub>3</sub>. Consequently, there is an increase of Coulomb repulsion between the electrons on Ru and O atoms. To minimize this, the structure distorts with the RuO<sub>6</sub> octahedra rotating around the 110 direction. To examine

TABLE I. Energies (eV) for SrRuO<sub>3</sub> and CaRuO<sub>3</sub> in their experimental structure, as well as SrRuO<sub>3</sub> in CaRuO<sub>3</sub> structure and vice versa.

Spin configuration	SrRuO <sub>3</sub> (in expt. structure)	CaRuO <sub>3</sub> (in expt. structure)	SrRuO <sub>3</sub> (in CaRuO <sub>3</sub> structure)	CaRuO <sub>3</sub> (in SrRuO <sub>3</sub> structure)
Ferromagnetic	-139.158	-141.070	-136.721	-140.260
Nonmagnetic	-138.979	-141.053	-136.721	-139.963
A-AFM	-139.057	-141.071	-136.723	-140.118
C-AFM	-139.024	-141.056	-136.721	-140.036
G-AFM	-138.984	-141.065	-136.722	-139.986

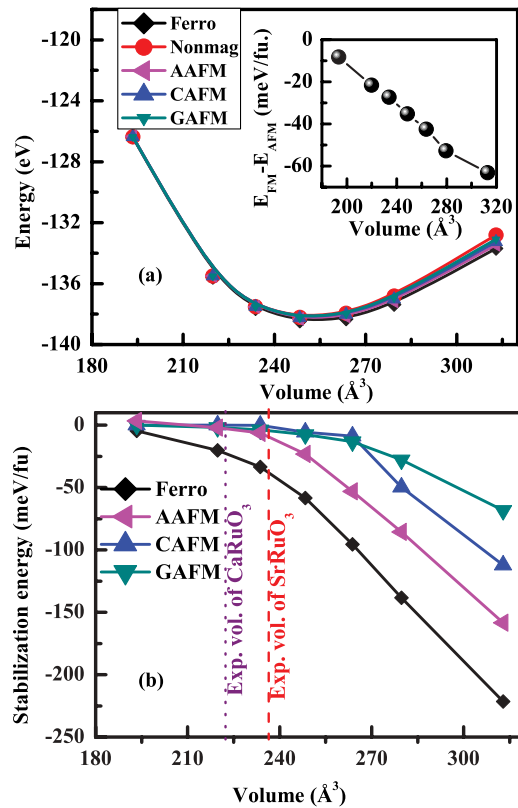


FIG. 1. (Color online) (a) The variation in energy with volume for different magnetic configurations of SrRuO<sub>3</sub>. Inset shows the energy difference between FM and competing AFM configuration. (b) The same energies plotted with respect to the nonmagnetic energy. In these calculations all atoms are at ideal perovskite lattice positions.

the consequences of this effect referred to as the GdFeO<sub>3</sub> distortion we have considered the cubic ideal perovskite unit cell for SrRuO<sub>3</sub> and appropriately rotated the RuO<sub>6</sub> octahedra. As a consequence of the rotation one has an increase in the Ru-O bond length with apical and basal oxygen atoms as shown in Fig. 2(a). This distortion, makes the Ru-O-Ru angle deviate from 180° as shown in Fig. 2(b) as a function of the rotation angle  $\theta$ . The elongation of the Ru-O bond length as well as the deviation in Ru-O-Ru angle results in a decrease in the one-electron band energy. This is compensated by a reduction in the Coulomb repulsion energy. These two competing factors result in the system favoring a distorted structure, where the total energy is found to be lowest for a rotation angle of 11° for SrRuO<sub>3</sub> as shown in Fig. 3(a) and in its inset. This is in reasonable agreement with the experimentally observed value of 166° for the Ru-O-Ru angle and is independent of the magnetic structure.

The FM metallic state derives its stability from an increased bandwidth of the 4d band. The distortion, however, reduces the effective hopping interaction between the Ru sites, and therefore the bandwidth. While magnetism gets destabilized at large  $\theta$ , we examined the dependence of the stability of the FM state on  $\theta$ . Model calculations carried out for systems which had  $e_g$  electrons at the fermi level found a  $\cos^2 2\theta$  dependence. This emerges from the dependence of the hopping integral between nearest neighbor transition metal sites on angle. A consequence of the prediction is that  $T_c$  is expected to the maximum

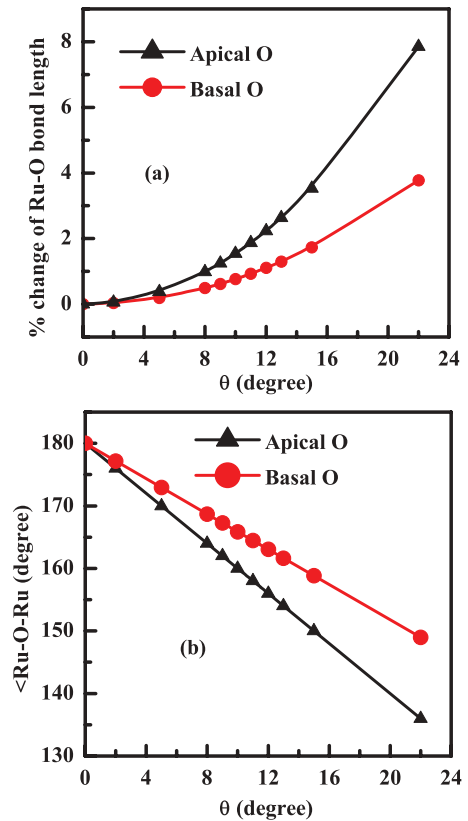


FIG. 2. (Color online) The variation of (a) the Ru-O bond length and (b) the Ru-O-Ru bond angle as a function of the rotation angle  $\theta$ . A cubic unit cell with a volume of SrRuO<sub>3</sub> is considered here, on which GdFeO<sub>3</sub> distortions are applied.

when the TM-O-TM angle is 180° and decreases for deviations away from it. The variation in the nearest neighbor exchange interaction strengths between Ru atoms in the  $xy$  plane ( $J_1$ ), Ru atoms in the  $z$  direction ( $J_1'$ ) as well as the second neighbor strengths  $J_2$  are plotted in Fig. 3(b) as a function of  $\theta$ . Almost all exchange interactions are FM, with the surprise being the increase in  $J_1', J_1$  for  $\theta$  less than 8°. The effective  $J_0$  (related to the  $T_c$  up to a multiplicative factor) is computed as  $\sum_i Z_i J_i$  where  $Z_i$  is the coordination associated with  $i^{\text{th}}$  neighbor. An increase from 88.3 to 98 meV is found for the same change in  $\theta$ . This effect is traced back to Fig. 2 where in addition to the decrease in the Ru-O-Ru angle that we find in panel (b), we also find an increase in the Ru-O bond lengths as a function of  $\theta$  in panel (a). The latter effect dominates and leads to the increase in the exchange splitting as a function of the  $\theta$ . For rotation angles greater than 8° we find the expected decrease in all exchange interaction strengths. We also examined the dependence of  $J_0$  on  $\theta$  in the window that it decreased. The decrease is much faster than the  $\cos^2 2\theta$  [dotted line in the inset of Fig. 3(b)]. At  $\theta = 17^\circ$  which corresponds to the  $\theta$  of CaRuO<sub>3</sub>, we still find an FM state to be stabilized. Hence, GdFeO<sub>3</sub> distortions alone do not destabilize ferromagnetism in CaRuO<sub>3</sub>.

We have performed similar calculations as a function of  $\theta$  for CaRuO<sub>3</sub> for the experimental volume for CaRuO<sub>3</sub>. The total energy shows a minimum at an angle of 17° [Fig. 4(a)]. The position of the energy minimum is found to be sensitive both to the atom at the A site and the volume. This is indeed

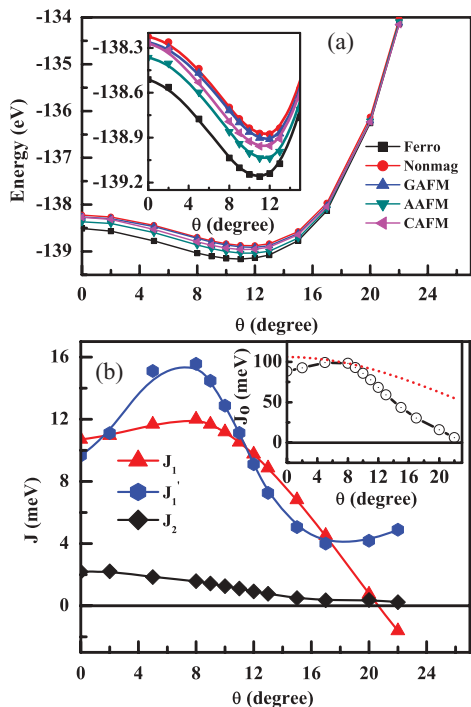


FIG. 3. (Color online) (a) The variation in energy as a function the GdFeO<sub>3</sub> distortion angle  $\theta$  for SrRuO<sub>3</sub>. The inset shows the magnified view near the energy minima. (b) The different exchange interaction strengths as a function of  $\theta$  and the total exchange interaction strength  $J_0$  is shown in the inset. The dotted line indicates the behavior of  $J_0 = A \cos^2(2\theta)$ . In these calculations we have considered a cubic cell with volume equal to that for SrRuO<sub>3</sub> on which GdFeO<sub>3</sub> distortions are applied.

what one expects based on the discussion of the microscopic interactions that drive the GdFeO<sub>3</sub> distortion. The energy difference between the FM state and the competing AFM state (A-AFM) [inset of Fig. 4(a)] indicate that for  $\theta \geq 16^\circ$  the values are within the error bars of our calculation. One finds similar trends in  $J_1$ ,  $J_1'$ , and  $J_2$  [Fig. 4(b)] as found for SrRuO<sub>3</sub> with a reduction in  $J_0$  to 15 meV from 30 meV found for SrRuO<sub>3</sub> in Fig. 3.

In addition to the GdFeO<sub>3</sub> distortion that we have considered, usually one has a rotation about the  $z$  axis. Considering this we obtained an energy reduction of 86 meV for the lowest energy of Fig. 4(b) ( $\theta = 17^\circ$ ). This is still almost one eV larger than the energy of the experimental structure (Table I). We then carried out a structural optimization and obtained an energy reduction of 0.99 eV, which arose from the displacement of the Ca atom from its ideal position. The origin of the displacement of the Ca atoms from their ideal position is easy to understand. With increasing GdFeO<sub>3</sub> distortion, the O atoms move closer to the Ca atoms, with a component of the energy stabilization arising from increased Ca-O hybridization.<sup>17,18</sup> The decrease in distance between Ca and O, however, increases the electrostatic repulsion between the electrons on Ca and O. The Ca atoms therefore displace and lower the energy of the system. The Sr displacements in SrRuO<sub>3</sub> are much smaller as it has a smaller GdFeO<sub>3</sub> distortion.

Thus, the combined effect of the GdFeO<sub>3</sub> distortion and volume are primarily responsible for the observed loss of long-

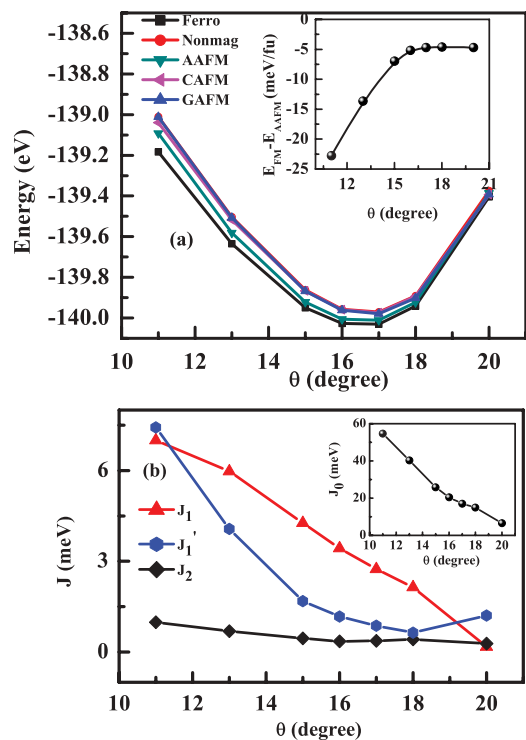


FIG. 4. (Color online) (a) The variation in energy as a function of the GdFeO<sub>3</sub> distortion angle  $\theta$  for CaRuO<sub>3</sub> with the energy difference between FM and A-AFM spin configuration shown in the inset. (b) The variation of different exchange interaction strengths and  $J_0$  (inset) as a function of  $\theta$ . Here we have considered a cubic cell with volume of CaRuO<sub>3</sub> on which GdFeO<sub>3</sub> distortions are applied.

range magnetic order in CaRuO<sub>3</sub> with the energy difference between FM and A-AFM being within our error bars, and C-AFM and G-AFM lying 14 meV higher. Other distortions bring all magnetic states very close as seen in Table I. The increased distortion reduces the bandwidth and hence makes the system more correlated. However, the loss of long-range magnetic order is because of the collapse of all exchange interaction strengths to very small values for large  $\theta$  as a result of which long-range magnetic order cannot be sustained in CaRuO<sub>3</sub>.

#### IV. CONCLUSION

We have studied the variation of the ferromagnetic stability as a function of the GdFeO<sub>3</sub> distortion in two prototypical  $I_{2g}$  systems CaRuO<sub>3</sub> and SrRuO<sub>3</sub>. An increase in ferromagnetic transition temperature is found initially with distortion, followed by the expected decrease. The functional form of the decrease in  $T_c$  cannot be fit to the expression  $\cos^2(2\theta)$  that one encounters for  $e_g$ -electron systems and exhibits a much faster decrease. The absence of long-range magnetic order in CaRuO<sub>3</sub> is traced to the collapse of all exchange interactions to very small values arising primarily from the smaller A ion induced volume reduction and RuO<sub>6</sub> octahedra rotation.

#### ACKNOWLEDGMENTS

S.M. thanks the Council of Scientific and Industrial Research, India for fellowship. P.M. and D.D.S. thank the Department of Science and Technology, Government of India.

\*Corresponding author: priya.mahadevan@gmail.com

- <sup>1</sup>P. B. Allen, H. Berger, O. Chauvet, L. Forro, T. Jarlborg, A. Junod, B. Revaz, and G. Santi, *Phys. Rev. B* **53**, 4393 (1996).
- <sup>2</sup>G. Cao, S. McCall, M. Shepard, J. E. Crow, and R. P. Guertin, *Phys. Rev. B* **56**, 321 (1997).
- <sup>3</sup>R. Vidya, P. Ravindran, A. Kjekshus, H. Fjellvag, and B. C. Hauback, *J. Solid State Chem.* **177**, 146 (2004); A. Callaghan, C. W. Moeller, and R. Ward, *Inorg. Chem.* **5**, 1572 (1966).
- <sup>4</sup>P. Khalifah, I. Ohkubo, H. Christen, and D. Mandrus, *Phys. Rev. B* **70**, 134426 (2004); Y. S. Lee, J. Yu, J. S. Lee, T. W. Noh, T.-H. Gimm, H.-Y. Choi, and C. B. Eom, *ibid.* **66**, 041104(R) (2002).
- <sup>5</sup>H. Nakatsugawa, E. Iguchi, and Y. Oohara, *J. Phys. Condens. Matter* **14**, 415 (2002).
- <sup>6</sup>M. V. Rama Rao, V. G. Sathe, D. Sornadurai, B. Panigrahi, and T. Shripathi, *J. Phys. Chem. Solids* **62**, 797 (2001); International Crystal Structure Database (ICSD) No. 51291.
- <sup>7</sup>P. Mahadevan, F. Aryasetiawan, A. Janotti, and T. Sasaki, *Phys. Rev. B* **80**, 035106 (2009).
- <sup>8</sup>I. I. Mazin and D. J. Singh, *Phys. Rev. B* **56**, 2556 (1997).
- <sup>9</sup>G. Santi and T. Jarlborg, *J. Phys. Condens. Matter* **9**, 9563 (1997).
- <sup>10</sup>K. Maiti, *Phys. Rev. B* **73**, 235110 (2006).
- <sup>11</sup>J. L. Garcia-Muñoz, J. Fontcuberta, M. Suaaidi, and X. Obradors, *J. Phys. Condens. Matter* **8**, L787 (1996).
- <sup>12</sup>G. Kresse and J. Furthmüller, *Phys. Rev. B* **54**, 11169 (1996).
- <sup>13</sup>P. E. Blochl, *Phys. Rev. B* **50**, 17953 (1994); G. Kresse and D. Joubert, *ibid.* **59**, 1758 (1999).
- <sup>14</sup>S. Blundell, *Magnetism in Condensed Matter* (Oxford University Press, Oxford, 2001).
- <sup>15</sup>P. Mahadevan, I. V. Solovyev, and K. Terakura, *Phys. Rev. B* **60**, 11439 (1999).
- <sup>16</sup>S. Middey, P. Mahadevan, and D. D. Sarma, *AIP Conf. Proc.* **1003**, 148 (2008).
- <sup>17</sup>J. B. Goodenough, *Magnetism and the Chemical Bond* (Interscience, New York, 1963); *Prog. Solid State Chem.* **5**, 145 (1971).
- <sup>18</sup>E. Pavarini, S. Biermann, A. Poteryaev, A. I. Lichtenstein, A. Georges, and O. K. Andersen, *Phys. Rev. Lett.* **92**, 176403 (2004); E. Pavarini, A. Yamasaki, J. Nuss, and O. K. Andersen, *New J. Phys.* **7**, 188 (2005).